nature communications

Article

https://doi.org/10.1038/s41467-025-58377-2

Microecology in vitro model replicates the human skin microbiome interactions

Received: 6 May 2024

Accepted: 20 March 2025

Published online: 31 March 2025

Check for updates

Pan Wang[1,4], Huijuan Li[1,4], Xingjiang Zhang[1], Xiaoxun Wang[1], Wenwen Sun[1], Xiaoya Zhang[1], Baiyi Chi[1], Yuyo Go[2], Xi Hui Felicia Chan[3], Jianxin Wu[1,4] ✉ & Qing Huang[1] ✉

Skin microecology involves a dynamic equilibrium among the host, microbiome, and internal/external environments. This equilibrium, shaped by multifactorial interactions, reflects individual specificity and diversity. Creating a replicable in vitro skin microecological model is highly challenging. Here, we introduce a mimicked stratum corneum microecology model (SCmic). It uses light cured crosslinked hydrogels as a scaffold and moisture source, and nonviable epidermal cells as the main nutrient. This setup establishes a suitable, stable, and reproducible microecology for microbiome colonization. Notably, it replicates the normal/oily skin microbiota with no significant differences from the original native microbiota at the genus level. Simultaneously, we have developed a standardized human skin microbiota model (Hcm), featuring seven dominant strains that form a representative microbial community. The models provide highly convenient approaches for exploring the intricate mutual interactions among skin microecology, influence of microbiota on skin health, and metabolism of chemical substances by microbiota.

As the largest organ of the human body, skin is colonized by diverse commensal microbes and serves as a microbial barrier to prevent the invasion of pathogens[1,2]. Many skin conditions are associated with an imbalance in the skin microbiome, for example common acne[3], atopic dermatitis[4] and sensitive skin[5]. Manipulating the human skin microbiome to address skin conditions has become a hot topic[6]. At the same time, the interaction between skin microbes and transdermal drugs, cosmetics and devices used on the skin cannot be ignored. However, it is a significant challenge to build a model that can reliably reproduce a complex host environment to evaluate microbial regulation[7]. The diversity of bacterial communities is influenced by the ecologically distinct microenvironments present on the skin, such as sebaceous, moist, and dry areas[8]. Sebaceous glands secrete the lipid-rich substance sebum, and provides relatively anoxic sites. The lipophilic anaerobe *Cutibacterium acnes* predominates in these sites, while *Corynebacteria* species and *Staphylococci* species predominated in moist sites[9]. So far, in vitro skin microbiome models have had difficulty mimicking the physiological and topographical niches in the skin.

In traditional culture-based environments, only a minority of the skin bacteria are able to thrive[10], with particular difficulty in maintaining the culture of anaerobes to replicate the skin microbe diversity. As skin microbiota has adapted to utilize the sparse nutrients available on the skin[11], in vitro skin microbiome models should also be nutritionally deficient. There have been several trials looking into the suitable platform for skin microbiota to colonize[12–15]. Among those, Reconstructed Human Epidermis (RHE) has been the most successful one as the RHE is generated from human stem cells and cultured on an air-liquid-interface, lacking the histological, physiological, and immunological complexity of human skin[7]. RHE has been applied for skin microbiology assays in cosmetic and clinical trials[16,17]. However, besides the cost and uncontrollable batch variation to produce RHE, the microbiome build on RHE couldn't recapitulate the native

[1]Skin Health and Cosmetic Development & Evaluation Laboratory, China Pharmaceutical University, Nanjing 211198 Jiangsu, China. [2]Department of Engineering Science, University of Oxford, Parks Road, Oxford OX1 3PJ, UK. [3]Department of Medicine, Waikato hospital, 183 Pembroke Street, Hamilton 3204, New Zealand. [4]These authors contributed equally: Pan Wang, Huijuan Li, Jianxin Wu. ✉e-mail: wujianxin@cpu.edu.cn; huangqingcpu@163.com

microbiota well and was not conducive to the study of aerotolerant anaerobes like *C. acnes*[7]. Although RHE can mimic the architecture of the human epidermis to a certain extent through air-liquid differentiation, it may be topographically different from native skin, which leads to the imprecise growth of anaerobic bacteria.

Skin microbiota mainly resides in the upper half of the stratum corneum. Using stratum corneum-like materials as a model for studying the microbiota has been considered as a suitable method[18]. The stratum corneum is the top layer of human skin, separating the living cell layer of the skin epithelium from the surface microbiota. It provides a physical barrier for microbiota to invade the skin[19]. Commensal bacteria that stay on the surface of the skin do not interfere directly with skin homeostasis to cause skin problems. It is only when the skin barrier is broken that the bacteria can cross the epidermal barrier and cause an inflammatory response[19,20]. Our previous study found that the crosslinked hydrogel obtained by light curing had similar mechanical properties to native skin, which could support the growth and proliferation of skin cells[21].

In this work, we developed a three-dimensional (3D) stratum corneum microbiome model (SCmic) designed to support the colonization and manipulation of universal microbial communities. Unlike living skin models, SCmic consists solely of a composition of photocuring crosslinked hydrogels (glycidyl methacrylate hyaluronic acid, GMHA) used as the scaffold, along with nonviable HaCaT and sebaceous cells serving as nutrients. We used this hydrogel as a scaffold to construct a skin microbiome model, enabling reproducible and cost-effective skin microbiology assays. The SCmic model was designed to maintain stable major skin commensals and allow co-survival of multiple bacterial species, including anaerobic bacteria, by modifying the hydrogel's thickness. Native skin microbiota collected from healthy volunteers were inoculated onto the model, and after re-inoculation on day 2 and subsequent culture for four days, the microbiota composition remained comparable to the original microbiome, particularly for normal and oily skin types. The microbial community also exhibited resistance to disturbance, such as water washing, indicating stable colonization and homeostasis. To further simplify and standardize the model, we established a conserved skin microbiota model (Hcm) based on the SCmic, consisting of seven commonly abundant skin strains[22], as a representative of the whole microbiota community. We demonstrated that following the proposed protocol the Hcm-SCmic are stable and reproducible. We also demonstrated the metabolic functionality of the SCmic microbiome by confirming that α-arbutin and niacinamide could be hydrolyzed to hydroquinone and nicotinic acid in the model. This suggests that SCmic provides a useful and straightforward vector for screening drug-microbiome interactions. In addition, by modifying the nutritional environment with the addition of simulated sebum: linoleic acid, squalene or olive oil, we found a significant increase in the number of *C. acnes* and a decrease in the number of *Staphylococcus epidermidis* and *Staphylococcus aureus* compared to controls. These findings indicate that excessive sebum secretion may disrupt microbial balance and contribute to skin conditions such as acne. SCmic provides a robust tool for studying microbial interactions and evaluating potential interventions to regulate the human skin microbiome.

Results

Development of SCmic

Based our previous study[21], we selected the photocrosslinked hydrogels GHMA as the scaffold material for the model. The hydrogel exhibits porous properties and a morphological structure that mimics the invaginations and depressions found in skin (Fig. 1b), which are important for creating niche-specific microenvironments[23,24]. These properties are essential for maintaining the steady state of the microbiota in vitro, as they create a non-uniform oxygen content in the model (Supplementary Fig. 1a) that provides suitable conditions for the co-growth of microbiota, including bacteria found in relatively anaerobic environments.

The skin is nutrient-poor and acidic, which is unsuitable for rapid multiplication and growth of the microbiota[25]. The hydrogels could maintain the acidic pH (~ 6.8) of the model surface during the inoculation which is suitable for microbiota to survive and stabilize (Supplementary Fig. 2). The gel is infused with an amount of inactive HaCaT cells and sebaceous cells to provide key nutrients while naturally mimicking the skin's stratum corneum to support microbial cultures. In our model, the ratio of HaCaT cells to sebaceous gland cells is 9:1 to reflect the cellular composition of the epidermis, since 90% of the stratum corneum is composed of keratinocytes[26].

Growth of anaerobic (*C. acnes*) and aerobic (*S. epidermidis* and *S. aureus*) bacteria

Anaerobic bacteria, such as *C. acnes*, constitute a significant portion of the human facial skin microbiota[27] and are primarily recognized as opportunistic pathogens[28]. Therefore, when aiming to mimic a pathological microbiome, such as the facial microbiome of acne patients, it is essential to focus on the growth of anaerobic *C. acnes*[29]. We therefore first investigated whether the anaerobe microbiota *C. acnes* could colonize on the SCmic model. *C. acnes* were inoculated on the model for 48 h, and SEM detected that the bacteria colonized properly to form a biofilm (Fig. 1c, d). We also found that *C. acnes* grow predominantly around cells, suggesting that the main nutrient sources for microbial growth were nonviable HaCaT and sebaceous cells (Fig. 1f).

Similar to *C. acnes*, aerobic bacteria *S. epidermidis* and *S. aureus* were inoculated on the model, respectively. The growth of each bacterium on day 0, 1, 3, 5 and 7 was analyzed by extracting the DNA and performing propidium monoazide (PMA)-quantitative PCR (qPCR) analysis. Compared to the day 0, the number of microorganisms decreased slightly after inoculation on the model. However, the bacterial numbers stabilized within a certain range from day 1 to day 7 (Fig. 1e). This can be explained by the fact that the bacteria need some time to adapt to the new environment, and once equilibrium is reached, the SCmic model can provide a favorable micro-ecological environment to support their stable growth.

Co-growth of bacteria communities on SCmic model with different thickness

The distinct habitats of microbiota are determined by factors such as skin thickness, folds and the density of hair follicles and glands[25]. To verify, we inoculated two main skin commensals (*C. acnes*) and (*S. epidermidis*), as well as one relevant skin pathogen (*S. aureus*) together onto the model with two different thinness (20 μm and 50 μm) in a 5:4:1 ratio. It is known that *S. aureus* and *S. epidermidis* are aerobic or facultative anaerobic bacteria, while *C. acnes* is an anaerobic bacterium. We cultured them at 32 °C and the growth distribution of these bacteria was observed by confocal laser scanning microscopy (CLSM) with FISH staining after incubation at 32 °C for 48 h.

C. acnes, *S. epidermidis* and *S. aureus* showed similar biofilm localization patterns in the 20 μm SCmic model (Fig. 1g). The distribution of biofilm biomass increased and then decreased with increasing depth. The trend of biomass change with depth is shown in Fig. 1g. In the 50 μm SCmic model (Fig. 1h), it was observed that both orange (*C. acnes*) and green fluorescent (*S. epidermidis*) bacteria exhibited a comparable distribution at 0 ~ 40 μm, interspersed with a small number of red fluorescent (*S. aureus*) bacteria. At the depths of 40 ~ 50 μm the biofilm biomass of *S. epidermidis* was relatively reduced (Fig. 1h). The results demonstrated that the model could support the co-growth of aerobic and anaerobic bacteria very well and that the SCmic thickness between 20 and 40 μm was suitable for skin bacteria to inhabit.

https://doi.org/10.1038/s41467-025-58377-2

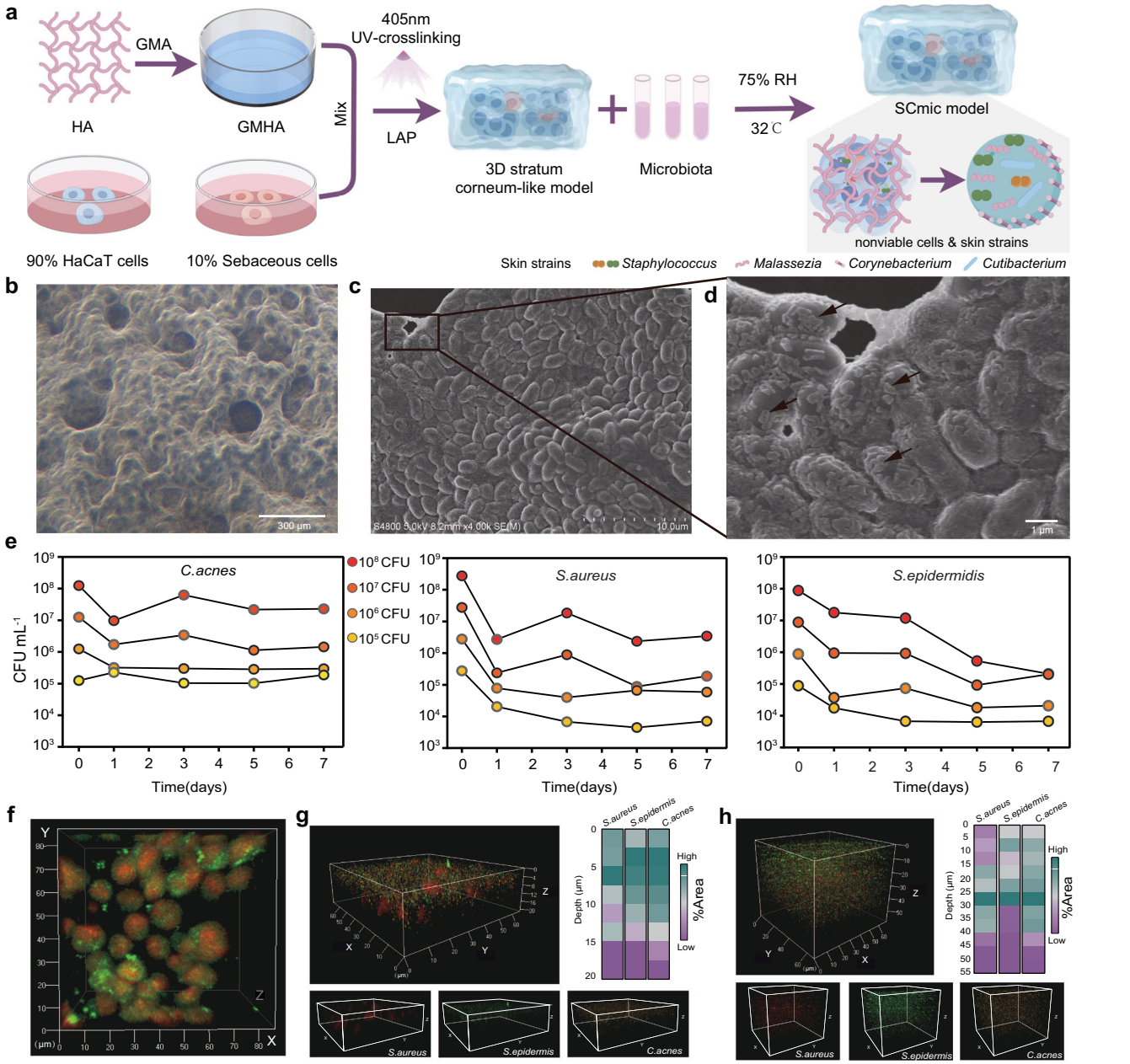

Fig. 1 | Establishment and evaluation of the SCmic model. a Workflow for the establishment of the SCmic model by Figdraw, which consists of a cross-linked hydrogel (GMHA), nonviable HaCaT and Sebaceous cells and microbiota. **b** Photograph of the model surface was taken with an inverted optical microscope (×4) (**c**) SEM plot of *C. acnes* biofilm generated after 48 h of incubation on the model. **d** Partial enlargement of Fig. c shows a large number of biofilms (arrows) in the surface of cells. **e** *C. acnes*, *S. aureus* and *S. epidermidis* inoculated on the model in different concentrations ranging from 10^4 to 10^8 colony-forming units (CFU) mL^{-1} and analyzed on days 1, 3, 5 and 7 by PMA-qPCR counting. **f** 3D reconstruction of confocal laser scanning microscopy (CLSM) images of the growth of bacteria on models with or without dead cells (green for live bacterial/red for dead cells). **g** 3D reconstructed CLSM Z-stacks of triple species biofilm images containing *S. epidermidis*, *S. aureus* and *C. acnes*. Bacteria were detected by FISH using *S. epidermidis*-specific (green), *S. aureus*-specific (red) and *C. acnes*-specific (orange) probes. SCmic model with a thickness of 20 μm. The heatmap represents the distribution changes of bacteria at different depths. **h** SCmic model with a thickness of 50 μm. 3D reconstructed CLSM Z-stacks of triple species biofilm images containing *S. epidermidis*, *S. aureus* and *C. acnes*. Bacteria were detected by FISH using *S. epidermidis*-specific (green), *S. aureus*-specific (red) and *C. acnes*-specific (orange) probes. The heatmap represents the distribution changes of bacteria at different depths. All microscopy experiments were performed in triplicate with similar results. Source data are provided as a Source Data file.

Reproducibility and temporal stability of the model

Having demonstrated that the model was suitable for aerobic and anaerobic microbials' co-colonization, we sought to assess whether more complex microbial communities could colonize and grow stably on the model, and what range of variability would result from the whole process. Using swabs, we obtained a native microbiota sample from the face of a healthy volunteer. After inoculation on day 0 and incubation for 5 days, the community structure changed (Fig. 2a, anosim, $p = 0.102$), and the microbial diversity decreased (Fig. 2b). However, by days 3 to 5, the bacterial community stabilized (Fig. 2a, anosim, $p = 0.903$), though with reduced diversity compared to the pre-incubation period. We further evaluated the microbial communities using a phylogeny-based metric (weighted Unifrac), where a smaller Unifrac distance indicates higher similarity between microbial communities. As shown in Fig. 2c, the microbial communities on the third day were similar to those on the fifth day. This suggests that the

https://doi.org/10.1038/s41467-025-58377-2

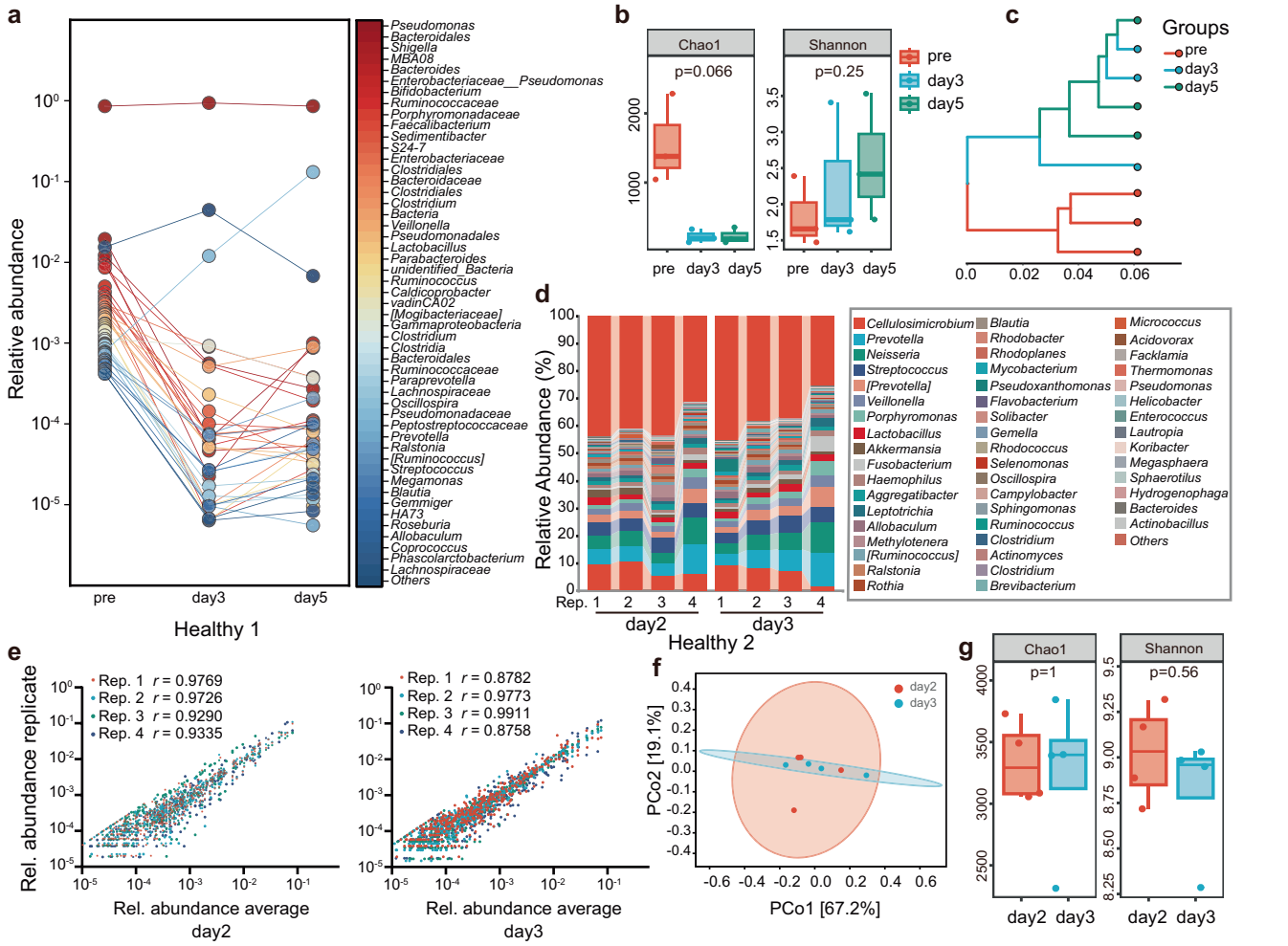

Fig. 2 | The skin microbiome can maintain community ecological stability on the model. a The bubble chart shows the distribution of the top fifty genera biomass in relative abundance in the model for pre-culture, and after 3 and 5 days of culture. Each dot is an individual strain, the collection of dots in a column represents the community at a single group, $n = 3$ biologically independent microbiomes. **b** Chao1 and Shannon indices of alpha diversity. The Kruskal-Wallis rank-sum test and Dunn's test were used as post-hoc tests to verify the significance of the difference. The boxplots denote the median with a quartile range (25–75%), and the length of whiskers represents 1.5× the IQR. $n = 3$ biologically independent microbiomes. **c** UPGMA phylogenetic tree constructed based on weighted UniFrac distances. **d** The composition bar plot shows the distribution of microbiome genera-level biomass in the model for 2 and 3 days of culture, $n = 4$ technical replicates. **e** Communities generated from the same inoculum ($n = 4$ technical replicates) have a nearly identical composition at day 2 and day 3, the color of each circle represents the corresponding genus, Pearson's correlation coefficient r of corresponding genus between average and technical replicate relative abundance (log10 rel. ab.). **f** Principal coordinate analysis (PCoA) plot based on weighted Unifrac. **g** Boxplots of pairwise comparison of the treatment alpha diversity indices using the Kruskal-Wallis rank-sum test and Dunn's test were used as post-hoc tests to verify the significance of the difference. The boxplots denote the median with a quartile range (25–75%), and the length of whiskers represents 1.5× the IQR. $n = 4$ technical replicates. Source data are provided as a Source Data file.

model has the ability to maintain a stable structure of the skin microbiota.

The skin microbiota of healthy individuals typically remains stable for up to two years[24]. Elizabeth K. et al.[30] also found that skin microbiota similarity is much higher over 24 h than over 3 months. Therefore, we chose 24-h intervals to assess whether the microbial communities colonizing the model remained relatively stable over time. We got the native microbiota sample by swabs method from the face of a healthy normal skin volunteer. The sample was separated in 8 replicates and inoculated on the SCmic models respectively. Cultured microbiota on the day 2nd and 3rd were analyzed by 16S rRNA sequencing to evaluate the growth stability of the microbiota.

The relative abundance of genus after 48 h and 72 h inoculation indicated that the flora communities reached a relatively stable configuration (Fig. 2d). Overall, the difference within the groups (day 2nd and 3rd) were relatively small, reflecting the good reproducibility of the model (Fig. 2e, $r > 0.85$). Moreover, there were no significant differences from phylum to family to genus between the two groups (Supplementary Fig. 3). Additionally, the overall composition of the two microbiota groups was highly similar (ANOSIM, weighted Unifrac, $p = 1$), as visually evident from the principal coordinate analysis (PCoA) plot, which shows no distinct separation between the groups (Fig. 2f). Furthermore, there were no significant differences in alpha diversity, as measured by the Chao1 and Shannon diversity indices (Fig. 2g, $p > 0.05$). Taken together, these results show that the method has acceptable variation, and the model is able to support the growth of complex skin microbiota with a high degree of temporal stability.

Replication of the native skin microbiota on the SCmic model

To assess the replicability on the SCmic model in terms of entire skin microbiota community formation, we conducted consecutive inoculation of the microbiotas obtained from normal, oily, and dry skin volunteers on the model, respectively. As observed previously, the bacterial population and community diversity on the day 3 were very

different from the original (Fig. 2a), as the bacteria needed time to adapt to their new environment. To address the issue, we decided to reinoculate the skin microbiota the next day, following the method of Gan et al. [31] To further demonstrate that skin microbiota can remain stable on the model, we included a control group with microbiota samples collected from the volunteer's face over four consecutive days (Fig. 3a). The results of 16S rRNA sequencing, shown in Supplementary Fig. 4, indicate that healthy human facial microbiota maintains a stable composition without large fluctuations. We reinoculated the native microbiota on the day 0 and 1, respectively, then cultured them continuously until day 4, with microbiota samples analyzed by 16S rRNA sequencing to evaluate the replicability of the microbiota on the SCmic model. The community characteristics were compared at 24-h (before re-inoculation) and 96-h of growth with those at day 0 (Fig. 3a).

The bar charts depicting genus-level biomass distribution showed that after 4 days incubation on the SCmic model, the microbiota composition of normal and oily skin returned to the pre-inoculation (day 0) level (Pearson's $r = 0.981$, $r = 0.994$), while the microbiota composition of dry skin exhibited more variability (Fig. 3b, Pearson's $r = 0.078$). Upon genus-level analysis of the normal facial microbiota, we observed a decrease in the relative abundance of *Propionibacterium* and an increase in *Micrococcus* in samples cultured for 24 h compared to the pre-culture counterparts. However, the successive inoculations of the microbiota onto the model restored the relative abundances of *Propionibacterium* and *Micrococcus* to the similar levels as in the pre-cultured state (Fig. 3b). The genus-level distribution of the microbiota before and after 4 days of incubation showed a high degree of consistency. Similarity test of the microbiotas before and after incubation was examined using the principal coordinate analysis (PCoA) and ANOSIM analysis[32]. The PCoA analysis indicated a clear separation at 24 h, while no sharp separation between 0 h and 96 h for the microbiota from the normal skin (Fig. 3c). Consistently, ANOSIM results reinforced this similarity pattern, demonstrating that the microbiota structure underwent significant alteration at the 24-h culture period (anosim, $p < 0.05$, Fig. 3g). However, upon reinoculation and extending the cultivation to 96 h, there was no statistically significant difference detected between the original and 96-h microbiota structures (anosim, $p > 0.05$).

Subsequently, we compared the microbiota derived from different skin conditions. The microbiota from oily skin exhibited a similar pattern to that of the normal skin, showing significant alterations at 24-h of inoculation but returning to the pre-inoculation levels after 96-h of culture by re-inoculations (Fig. 3d, g). PCoA analysis demonstrated that, following 96-h of cultivation, the microbiota originating from the normal and oily skin closely resembled their initial inoculation, clustering tightly together (Fig. 3c, d, f). In contrast, the microbiota cultured from the dry skin was initially clearly separated from its pre-inoculation state, but the dispersion tended to decrease over time, indicating a gradual convergence of the microbiota to its original state. (Fig. 3e, f). The results show that the SCmic model is more similar to the microecology of normal and oily skin, but is not entirely suitable for the growth of dry skin microbiota.

On the other hand, the microbiota sourced from the normal and oily skin were distinctly separated, indicating that the SCmic model could reflect the difference well (Fig. 3h, i). The richness and diversity of these restored microbial communities were maintained well in the models (Fig. 3h, i). In addition, the microbial community composition remained relatively stable even up to 7 days in the SCmic model (Supplementary Fig. 5).

The results show us the potential for establishing individual-specific skin microbiota models or representative pathogen models for related study.

Microbiota colonization against interruption

To test whether the skin microbiota colonized on the SCmic model exhibits resistance to some external influences, we rinsed the model with PBS to simulate daily face washing. After inoculating the skin native microbiota on the SCmic, we washed the model at 48 h and then further incubated it for another 24 h. The DNA was extracted for sequencing at 48 h and at 72 h for both the Control and Wash groups (Fig. 4a).

Compared to the Control group, the microbial diversity (Chao1 index) and species richness (Shannon index) tended to decrease in the Wash group (Fig. 4c). However, for genera with higher relative abundance, most microorganisms did not show significant changes at the genus level (Fig. 4b).

To further analyze the similarities of overall microbial composition between the Wash and Control groups, PCoA analysis based on the weighted Unifrac distance was applied. The results (Fig. 4d) showed that the microbial communities were closely clustered, with no significant differences before and after washing (Con-48h vs Wash-48h, anosim, $p = 0.057$). After an additional 24 h of cultivation, the microbiota composition became even more similar (Con-72h vs Wash-72h, anosim, $p = 0.077$). Furthermore, we observed that the relative abundance of the genus of *Staphylococcus* and *Bacteroides* significantly increased for another 24 h incubation after washing (Fig. 4e). The results indicated that once the colonies reached a steady state, even if the microbiota was affected by external factors such as washing, the colony communities were able to recover again.

Constructing a human skin conserved microbiota (Hcm)

In order to simplify the process and reduce the variety we further established a conserved human skin microbiota model (Hcm) in a controlled setting on the SCmic. The microbiota consisted of the top six bacteria and one fungus (all commercially available) referred to the study by Zhiming Li et al.[22]. Although this conserved microbiota does not fully represent the entire ecological community, it is more suitable as a representative for some research as it encompasses a significant proportion (> 50%) of the skin microbiota and eliminates the potential influence of different skin states on the microbiota.

To ensure the viability of the cultured strains, we inoculated each strain from the frozen stock solution into the appropriate liquid medium and conducted regular passaging every 24 or 48 h. Prior to combining the individually cultured strains, we thoroughly rinsed each strain at least three times using a PBS solution. This ensured that the growth of the strains was not disrupted by the presence of other nutrients. Please refer to Fig. 5a for a visual representation of the inoculation process.

Stability of Hcm on SCmic model

The strains were then incubated for a total of 96 h, and DNA samples were extracted at 0, 24, 48, and 96 h for PMA-qPCR sequencing.

The colony-forming units (CFUs) of each strain at each time point are shown in Fig. 5b, while Fig. 5c displays the average relative abundance of each strain. Each dot represents an individual strain, and the collection of dots in a column represents the community of a single group, indicating the stability of community after 24 h, with the exception of *C. granulosum*, which showed relatively more variation. The relative abundance remained largely unchanged, with a Pearson's correlation coefficient consistently exceeding 0.95 when compared to the pre-colonization community at each time point (Fig. 5d). The degree of similarity of the technical replicates was significant high (Fig. 5e), suggesting that the errors introduced by the modeling process, DNA extraction, and qPCR assay could remain small enough to demonstrate the model as a stable and useful tool.

Influence of sebum on microorganisms in the Hcm model

Numerous studies have shown that acne is largely influenced by diet and over-secretion of sebum from the skin[33]. However, the correlating

https://doi.org/10.1038/s41467-025-58377-2

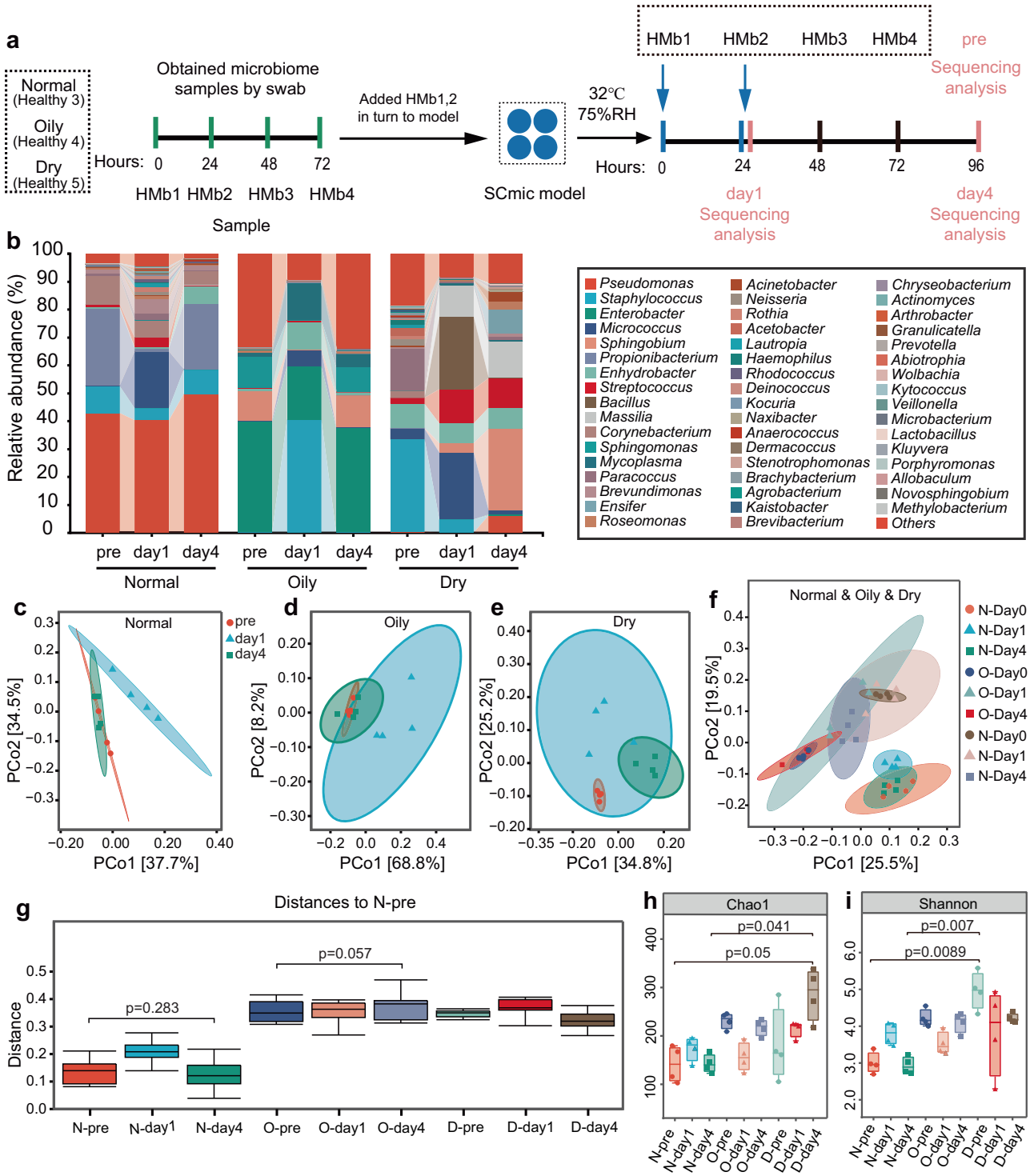

Fig. 3 | Replication of microbiota of different skin origins (Normal, Oily, Dry) on SCmic models. a Method for continuous inoculation of skin microbiota onto the model. **b** Compositional bar chart showing genus-level biomass distribution of the continuously cultured microbiome in the model. **c**–**e** Principal coordinate analysis (PCoA) plot (based on weighted Unifrac) of Normal, Oily and Dry microbiota cultured for 0, 24 and 96 h. **f** PCoA plots of Normal, Oily and Dry microbiota. **g** Analysis of similarities (Anosim) based on weighted UniFrac distance matrix showed differences between the microbiota of Normal, Oily and Dry for day0, day1 and day4. The boxplots denote the median with a quartile range (25–75%), and the length of whiskers represents 1.5× the IQR, $n = 4$ biologically independent microbiomes per group. **h** Chao1 richness estimators of Normal, Oily and Dry microbiota. The Kruskal-Wallis rank-sum test ($p = 0.0024$) and Dunn's test were used as post-hoc tests to verify the significance of the difference. The boxplots denote the median with a quartile range (25–75%), and the length of whiskers represents 1.5× the IQR, $n = 4$ biologically independent microbiomes per group. **i** Shannon diversity index of Normal, Oily and Dry microbiota. The Kruskal-Wallis rank-sum test ($p = 0.0016$) and Dunn's test were used as post-hoc tests to verify the significance of the difference. The boxplots denote the median with a quartile range (25–75%), and the length of whiskers represents 1.5× the IQR, $n = 4$ biologically independent microbiomes per group. Source data are provided as a Source Data file.

https://doi.org/10.1038/s41467-025-58377-2

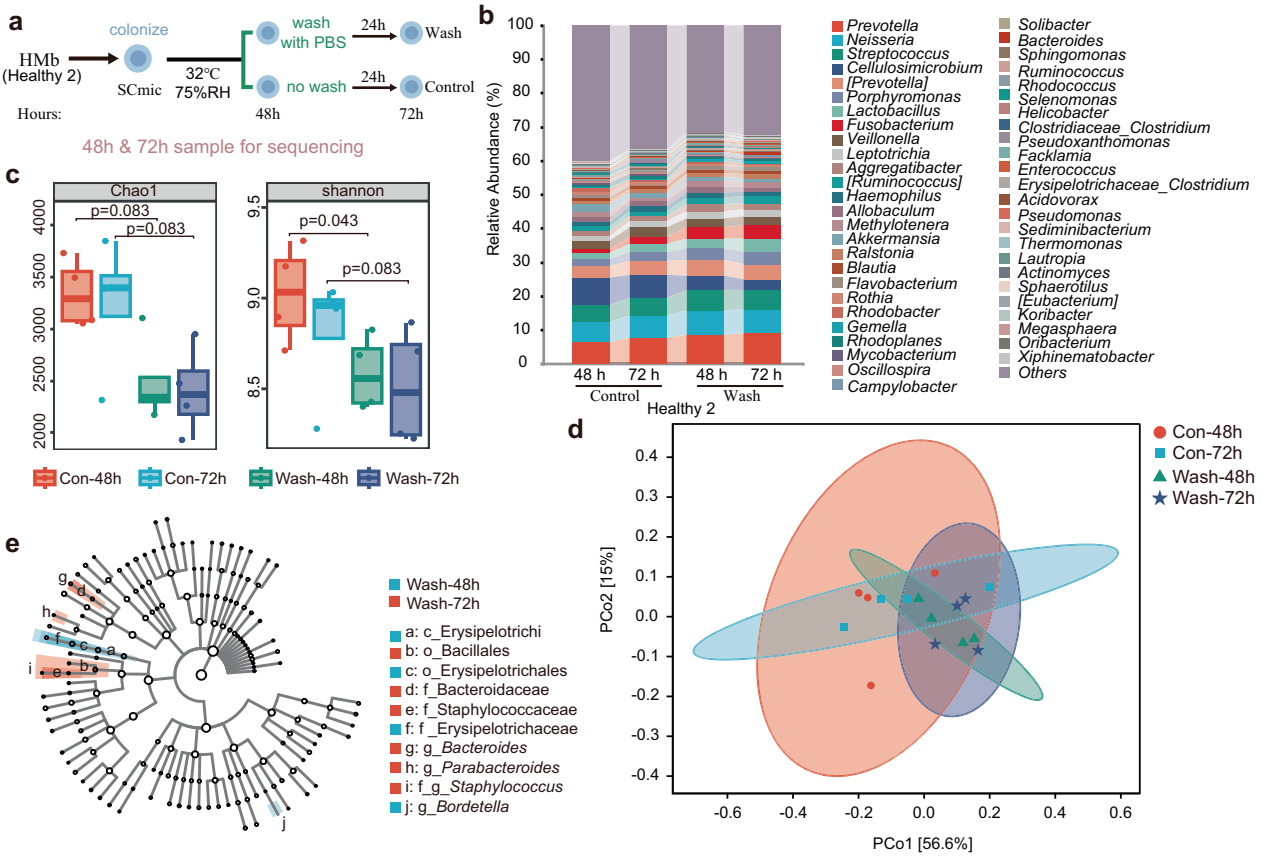

Fig. 4 | The skin microbiome has the ability to resist interference and metabolism on the model. a Schematic diagram of the PBS wash challenge experiment. **b** The composition bar plot shows the distribution of the top fifty genera biomass in relative abundance in the model. **c** Chao1 and Shannon indices of alpha diversity. The Kruskal-Wallis rank-sum test and Dunn's test were used as post-hoc tests to verify the significance of the difference, the boxplots denote the median with a quartile range (25–75%), and the length of whiskers represents 1.5× the IQR, Con-48h, $n = 4$ technical replicates; Con-72h, $n = 4$ technical replicates; Wash-48h, $n = 4$ biologically independent microbiomes; Wash-48h, $n = 4$ biologically independent microbiomes. **d** Principal coordinate analysis (PCoA) based on weighted Unifrac distance matrix showed differences between groups for Con-48h, Con-72h, Wash-48h and Wash-72h. Con-48h: Skin microorganisms are cultured on the model for 48 h; Con-72h: Skin microorganisms are cultured on the model for 72 h; Wash-48h: The skin microbiome were cultured on the model for 48 h and then rinsed three times with PBS; Wash-72 h: After rinsing with PBS, continue to culture the microbiome for 24 h. **e** The taxonomic clade shows the taxonomic hierarchical relationships of the main taxa in the wash and wash-24 h community, from phylum to genus (from inner circle to outer circle). Differences were identified by linear discriminant analysis (LDA) effect size analysis (LEfSe, LDA score >2). Blue and red nodes indicate that these taxa exhibit significant between-group differences and are more abundant in the grouped sample represented by that color. c: class; o: order, f: family; g: genus. Source data are provided as a Source Data file.

evidence between increased sebum secretion and microbiota abnormalities remains unclear. Therefore, we manipulated the nutrients by adding 2 mg of linoleic acid or squalene, or olive oil to represent three different kinds of hydrocarbons to simulate an excessive increase in sebum components in the model.

We added the above three oils respectively to the conserved Hcm model (Fig. 5f). After inoculation the relative abundance and the population of each strain in the experiment were analyzed (Fig. 5g). Interestingly, the addition of linoleic acid, squalene and olive oil significantly increased the relative abundance of *C. acnes* while reduced the relative abundance of *S. epidermidis* and *S. aureus* compared to the control group (Fig. 5h). However, no significant changes were observed in the remaining strains. Further analysis revealed that the numbers of *S. epidermidis* and *S. aureus* (Fig. 5i) decreased significantly, whereas other strains, including *C. acnes* reminded stable.

Taken together, our findings indicated that an excessive increase in sebum regardless of fatty acids, hydrocarbon oils or triglycerides led to a significant rise in the relative abundance of *C. acnes* by inhibiting the growth of *S. epidermidis* and *S. aureus*, consequently resulting in an abnormal community composition. These findings suggest that sebum plays an important role in shaping the composition and abundance of microbial communities.

Metabolism of arbutin and niacinamide by the Hcm model

The skin microbiome is known to be a micro-barrier that can metabolize certain harmful chemicals[34]. To assess whether the SCmic model maintains the function of skin microbiome in its interaction with xenobiotics, we tested arbutin and niacinamide, which are widely used in cosmetic products. The SCmic model was inoculated with the Hcm microbiota, 50 µL of arbutin and of niacinamide solution were added at 24 h time point to the model, respectively, then incubated for another 24 h. As shown in Fig. 6b, the microbiota was able to hydrolyze α-arbutin to hydroquinone. Molecular docking suggested that this may be attributed to the widely expressed α-glucosidase in the skin microbiota, with relatively low conformational energy of *C. acnes* α-glucosidase and arbutin being -6.9 kcal M^{-1} (Fig. 6c, d). Hydroquinone has strong skin lightening effect while also has high skin irritation and toxicity such as genotoxicity and nephrotoxicity.

Additionally, we assessed the interaction between niacinamide and the Hcm microbiota. As shown in Fig. 6e, the microbial community can hydrolyze niacinamide into nicotinic acid. It is known that gut

https://doi.org/10.1038/s41467-025-58377-2

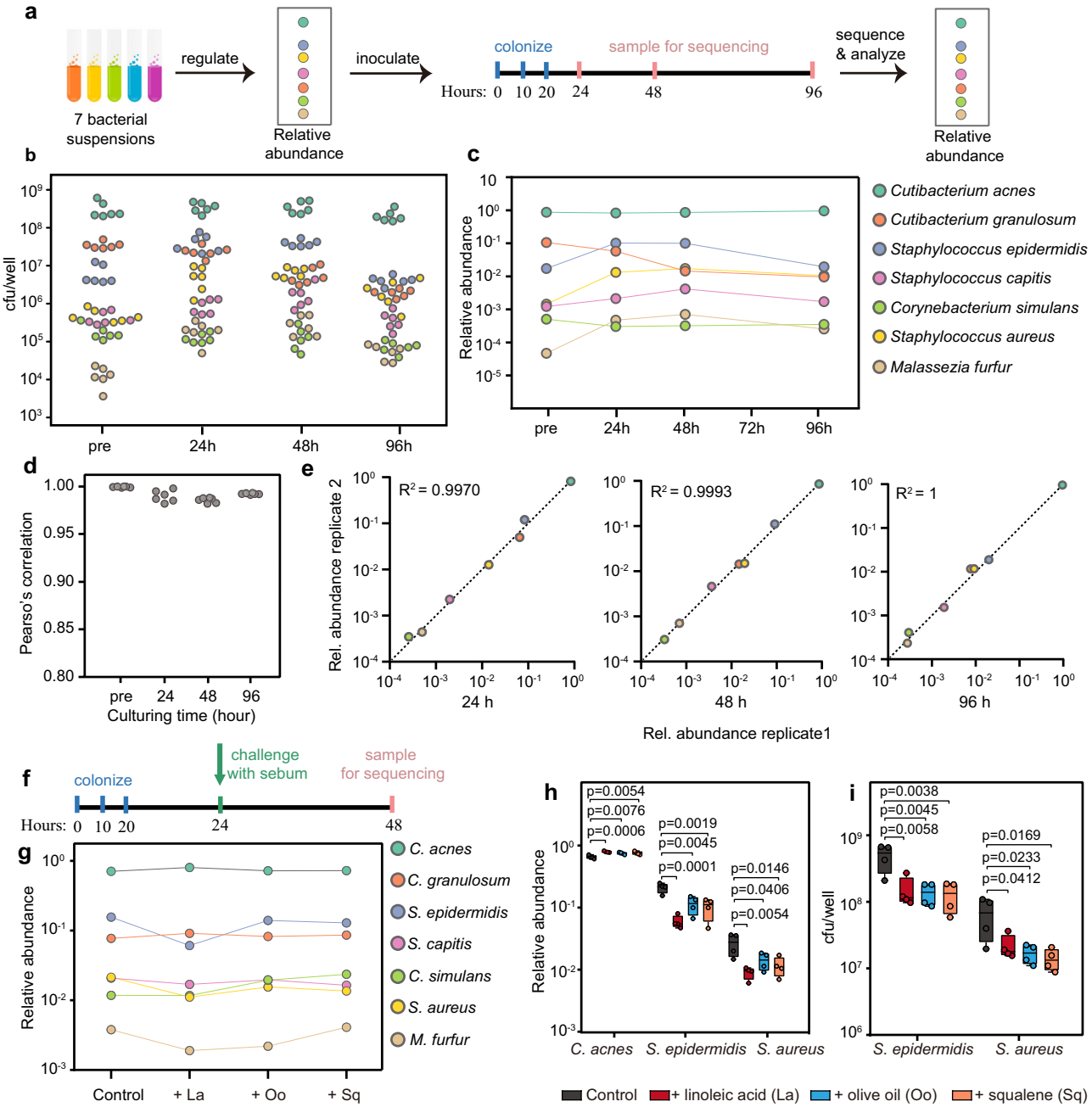

Fig. 5 | Constructing and maintaining stable conserved microbiota on SCmic models. a Schematic of the experiment. Frozen stocks of the 7 strains were used to inoculate separate cultures, which were then grown for either 24 or 48 h. After the incubation period, the strains were mixed together in specific ratios and moistened with PBS. The mixture was then inoculated onto the model surface, and the colonies were incubated at a temperature of 32 °C and a relative humidity of 75% for a duration of 24 to 96 h. At each time point, the colonies were collected, and the abundance of each strain was detected using PMA-qPCR. **b** Scatterplot of the number of seven strains at each time point. **c** Average relative abundances of the 7 strains at each time point, $n = 6$ technical replicates. **d** Pearson's correlation coefficient r between cultured microbiota at each time point and the average pre-colonization community. **e** Communities generated from the same inoculum have a nearly identical composition at 24, 48, 96 h, $n = 3$ technical replicates. **f** Schematic diagram of experiments in which sebum affects conservative microbiota. **g** Average relative abundances of the 7 strains at each time point with the impact of linoleic acid, squalene, and olive oil. **h** Significant effect of linoleic acid, squalene, and olive oil on the average relative abundances of *C. acnes*, *S. epidermidis* and *S. aureus*, the boxplots denote the median with a quartile range (25–75%), and the length of whiskers represents 1.5× the IQR, $n = 4$ biological replicates. **i** Significant effect of linoleic acid, squalene, and olive oil on the average number of *S. epidermidis* and *S. aureus*, the boxplots denote the median with a quartile range (25–75%), and the length of whiskers represents 1.5× the IQR, $n = 4$ biological replicates. Statistical significance was assessed using a one-way ANVOA. Source data are provided as a Source Data file.

microbiota promotes mammalian NAD metabolism by converting nicotinamide to nicotinic acid[35]. Our analysis revealed for the time that the skin microbiota may possess nicotinamidase (PncA), an enzyme responsible for this conversion. We further analyzed and determined multiple skin bacteria encoding the nicotinamidase PncA (Supplementary Table 1). Molecular docking demonstrated a favorable binding of *C. acnes* PncA and nicotinamide, with a conformational energy -3.9 kal M^{-1} (Fig. 6f, g). We know that nicotinic acid may cause facial skin tingling, itching, and flushing[36], so caution is advised when using niacinamide in skincare products.

https://doi.org/10.1038/s41467-025-58377-2

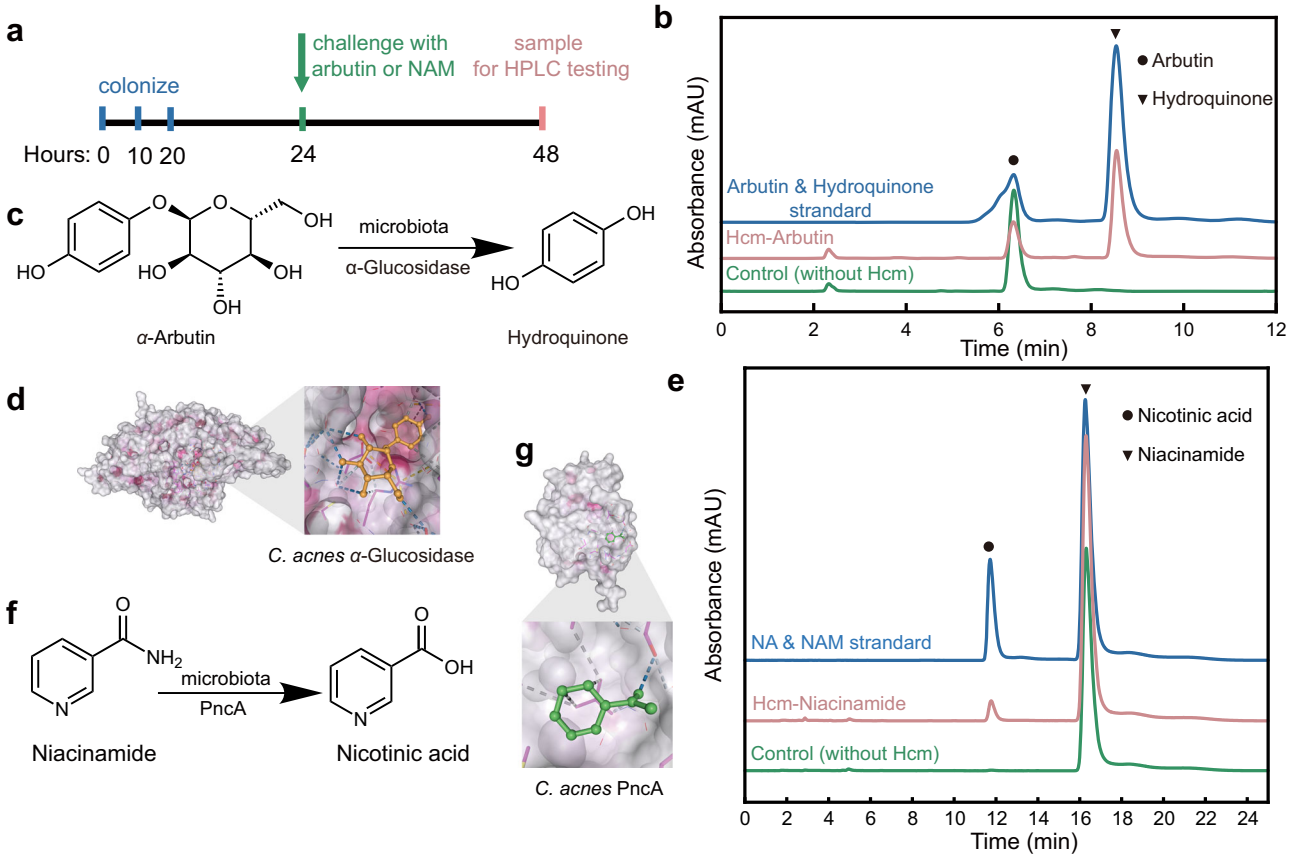

Fig. 6 | Skin microbiota (Hcm) in the model can metabolize arbutin and niacinamide (NAM) to hydroquinone and nicotinic acid (NA). a Schematic diagram of experiments on the metabolism of arbutin and niacinamide by skin microbiota. **b** High-performance liquid chromatography (HPLC) chromatogram of the reaction mixture of arbutin and Hcm in the model. Blue: Arbutin and Hydroquinone standard; Red: 24 h after incubation of arbutin with Hcm in SCmic model; Green: 24 h after incubation of arbutin without Hcm in SCmic model. **c** Structure of degradation products of α-Arbutin. **d** Molecular mechanical model of α-Arbutin binding to *C. acnes* α-Glucosidase. **e** HPLC chromatogram of the reaction mixture of niacinamide and Hcm in the model. Blue: niacinamide and nicotinic acid standard; Red: 24 h after incubation of niacinamide with Hcm in SCmic model; Green: 24 h after incubation of niacinamide without Hcm in SCmic model. **f** Structure of degradation products of niacinamide. **g** Molecular mechanical model of niacinamide binding to *C. acnes* PncA. Source data are provided as a Source Data file.

Discussion

The human skin hosts an extensive and diverse microbial community, with approximately 10^6 bacteria per square centimeter[1], and perturbations in this community have been linked to various skin conditions. Yet, the lack of highly reproducible and diverse in vitro skin microbiome models hampers related research of e.g. drug-microbiome interaction. Unlike the gut environment that favors bacterial growth, the skin's dry, salty, acidic, and nutrient-poor nature along with external factors like oxygen, moisture, and pH influence the skin microbial community[37,38].

Even in the presence of air and sunlight, many skin bacteria favor microaerophilic environments. Traditional nutrient-rich cultures may inadvertently promote microbiota adapted to laboratory conditions[2]. Bacteria residing on the skin derive nourishment from constituents of the stratum corneum, as well as sebaceous and skin secretions[1]. When introducing skin-derived microbiota into an in vitro culture media model, it becomes essential to consider the influence of nutrient availability on bacterial growth dynamics and the equilibrium of microbiota. Therefore, when studying the influence of external factors on the skin microbiome in vitro, it is necessary to establish a microbial model that can dynamically maintain stability rather than overgrowth, and simulate the growth state of microbiota on the skin.

Previously, it was virtually impossible to support all microbiota, aerobic and anaerobic, to maintain the same growth rate in an in vitro medium or environment. To address these challenges, we developed a SCmic model consisting of a photocuring crosslinked hydrogel (glycidyl methacrylate hyaluronate, GMHA) as a scaffold with inactive HaCaT and sebaceous cells as nutrients to mimic the microecological environment. This hydrogel can macroscopically simulate the complex topography of skin surface depressions and indentations. This approach provides a conducive environment for microbiota to actively acclimate to their surroundings. Rigorous validation attests to the model's ability to effectively uphold the composition of the skin microbiota, including both anaerobic and aerobic bacteria (Fig. 1g, h, Supplementary Fig. 6).

During our study, we observed that the composition of the microflora changed considerably when the microflora obtained from human facial skin was inoculated onto the model within the first 24 h, as the microflora needed time to adapt to the new environment. To aid and accelerate the colonization of the microbiota on the model, we inoculated the microbiota twice in succession and successfully replicated the skin microbiota on the model, especially replicating the microbiota from normal and oily skin.

Based on the results from Fig. 2a, we decided to reinoculate on day 1. In the Fig. 2a experiments, we observed that when microbiota was inoculated only on day 0 and left for 5 days, microbial diversity declined and community structure changed (anosim, $p = 0.102$). However, the bacterial communities stabilized between days 3 and 5 (anosim, $p = 0.903$), though with reduced diversity compared to the original community. In addition, we observed that the majority of

microbiota derived from human skin could colonize the model by day 5, with 88% of the top 50 most abundant genera establishing themselves. We speculate that the changes in community structure may be due to the loss of low-abundance genera or those that are more difficult to colonize (Fig. 2a). For example, low-abundance genera (< 1%) generally decreased from day 0 to day 3. Similar to previously reported results, when gut microbiota was introduced into germ-free mice, low-abundance members were more likely to disappear[39]. In such cases, a single inoculation of hard-to-colonize microbes could lead to more significant microbial community changes, and multiple inoculations in germ-free mice have been shown to improve this issue[31].

In addition, the SCmic model environment is not identical to the natural skin environment, and the initial inoculation may not provide optimal colonization conditions for all strains, which could lead to reduced diversity (Figs. 2b, 3h). After the initial inoculation of skin microbiota onto the model, changes in the model's pH and oxygen levels likely create an environment favorable for a second inoculation. The model's pH increases after inoculation (Supplementary Fig. 2), and a neutral pH is more conducive to the colonization of commensal bacteria compared to an acidic pH. Although the skin surface is often acidic, recent research by Fukuda et al.[40] found a pH gradient in the skin's stratum corneum, with the middle layers being acidic to serve as a barrier against pathogens, while the upper layers, influenced by microbial growth, tend to be neutral. The pH of the SCmic model shows a similar trend to the upper layers of the skin's stratum corneum. Furthermore, we also found that oxygen levels decreased and a non-uniform oxygen content existed within the SCmic model after the initial inoculation, supporting the coexistence of a diverse microbial community.

However, microbiota obtained from dry skin show some variation in replication. Dry skin is characterized by lower levels of sebum and moisture, whereas the SCmic model uses a hydrogel scaffold with high water content, predominantly free water. Further adjustments in humidity and other factors needs to be considered to establish a microecological environment suitable for the colonization of dry skin microbiota. Factors such as gel type, porosity, and crosslinking degree influence the free water content, which can be reduced by increasing the crosslinking degree or using a combination of gels. Besides dry skin, various pathological skin conditions, such as atopic dermatitis, psoriasis, acne, and seborrheic dermatitis, are often associated with specific skin areas with unique characteristics. We have found that extreme pH conditions and varying the amount of the cross-linking agent MBA can significantly affect bacterial colonization. Additionally, increasing the concentration of GMHA enhances gel stiffness, which can influence bacterial colonization (Supplementary Fig. 7). Future exploration of adjusting the model parameters to alter the physical state of the model may make it suitable for culturing microbiota from a broader range of skin types.

In our study, we chose the swab sampling method for its non-invasive nature, minimal disruption, and comfort for volunteers. While swabs may not fully represent the resident microbiota of the entire skin layer, they effectively capture the overall composition of the skin microbiota that can be maintained in our scaffold model. The study by Grice, E. A. et al.[41] suggests that swabs, scrapings, or punch biopsies are all sufficient to obtain a representative profile of the community members.

Many studies have shown that certain skin conditions are correlated with imbalances in the skin microbiome. For instance, acne is believed to be associated with sebum overproduction, altered keratinization, inflammation, and skin microbiota dysbiosis[42]. These imbalances in the skin microbiota can be attributed to various factors, including an oil-water imbalance in the skin[43], excessive cleaning, and the use of drugs and cosmetics[6]. Hence, our study assessed the ability of the model to respond when dealing with sebum overproduction. Our findings suggested that increased sebum leads to a significant increase in the relative abundance of *C. acnes*, which is consistent with previous studies[44]. However, further analyses revealed that increased linoleic acid, squalene, and triglycerides didn't directly affect the growth of *C. acnes*. Instead, they contributed to an imbalance in the microbiota by reducing the growth of *S. aureus* and *S. epidermidis*. Based on our findings, we can hypothesize that the imbalance of facial microbiota in acne patients is not solely related to the increase in *C. acnes*, but rather to the decrease in the proportion of other strains. Similar to the view of a small group of research in recent years, targeted therapies to maintain skin health may need to inhibit not only the growth of pathogenic bacteria, but also the growth of commensal bacteria[9,45]. Furthermore, our study demonstrated that changing the environment from dry to wet in the model leads to a significant increase in *Staphylococcus spp* (Fig. 4e), which is consistent with previous studies[9]. Further research is definitely needed on how extrinsic factors such as specific nutrients, pH, UV radiation, humidity and exogenous pathogens affect the growth of individual bacteria and the balance of the microbiota.

To date, the human gut microbiota is known to alter the pharmacological properties of more than 50 drugs[46] and the metabolic activity of the skin microbiota also affects topical medications. In certain instances, the efficacy, toxicity and teratogenicity of these microbial metabolites remained unrecognized until drugs were already on the market. Hydroquinone, owing to safety concerns, is no longer employed in cosmetic whitening formulations despite its proven skin-whitening efficacy[47]. In contrast, arbutin, possessing a similar chemical structure to hydroquinone, is considered a safe alternative and is currently utilized in commercially available skin whitening products. Bang et al. confirmed that β-arbutin can be hydrolyzed to hydroquinone by microbiota isolated from normal skin microbiota[48]. Our research demonstrates that α-arbutin can also undergo metabolism by skin microbiota, potentially due to the presence of glucosyl hydrolase enzymes. A search of the NCBI database, which contains sequences from completely sequenced *C. acnes*, *S. epidermididis*, *Malassezia restricta* and *Corynebacterium simulans* genomes, reveals the existence of over 20 glycoside hydrolase protein sequences. Niacinamide has been shown to have excellent safety profiles[49]; however, some individuals may experience stinging when using products containing niacinamide. We speculate that microbial conversion of niacinamide to niacin may be a major contributing factor.

An in vitro microbiome model should be a stable and useful vector for researchers to purposefully manipulate skin microbes for skin health related study. Therefore, in addition to replicating the entire skin flora, we have created a conserved skin microbiota model (Hcm), which is simpler and easier to construct. The capacity to manipulate and maintain microbiota composition in response to perturbations is crucial, especially as synthetic communities gain traction in microbiome research[50]. As progress is made towards constructing synthetic microbiome for both healthy and pathological states, our model will assume an increasingly pivotal role in future investigations. In addition, future studies can integrate in vitro cultured microbiota with 3D skin culture model to explore the interactions between the two and thereby understand the mechanisms by which skin microbial communities regulate physiological and pathological processes in the skin.

In conclusion, the intricate interplay between the skin and its microbiome presents complex challenges in in vitro modeling. The in vitro models we present address these challenges by providing a platform that mirrors the ecological landscape of skin corneum, facilitating investigations into microbiome interactions and responses to external factors. This advancement holds promise for enhancing our understanding of skin conditions and the development of targeted interventions.

Methods

Preparation of the GMHA and cell culture

Glycidyl methacrylate-HA (GMHA) conjugates were synthesized according to the method of Jennie Baier Leach et al.[51] with slight modifications. Briefly, 1.0 g HA (410 Kda, Jiangsu Haifei Biotechnology Co., Ltd.) was dissolved in 100 mL phosphate buffer (PBS, cat# G101, Vazyme, 10 mM, pH 7.4); 7.5 mL triethylamine (cat# 81101, Sigma), 7.5 g tetrabutyl ammonium bromide (cat# 301590, Sigma), and 7.5 mL glycidyl methacrylate (GM, cat# 151238, Sigma) were added separately, followed by a 44-h incubation at 20 °C. After the reaction, the reaction solution was transferred to a dialysis bag with molecular weight cut-off 3.5 KDa. After dialysis the reaction solution was freeze-dried to obtain GMHA freeze-dried product. The schematics of the chemical reactions is shown in Supplementary Fig. 8.

Secondary sebocytes were transfected with the pGMLV-SV40T-PURO lentiviral vector (cat# GM-0220LV06, Genomeditech) to generate the immortalized human sebocyte cell line (sebaceous cells)[52]. HaCaT (Meisen Cell Technology Co., Hangzhou, China) and sebaceous cells were expanded in DMEM (cat# CTCC-002-008, Meisen Cell Technology Co., Ltd.) with phenol red supplemented with 10% v v^{-1} heat-inactivated fetal bovine serum (FBS, cat# FS401-02, TransGen Biotech) and 1% v v^{-1} penicillin (10,000 units mL^{-1})/streptomycin (10 mg mL^{-1}) until 100% confluent. After removing the growth medium, cells were trypsinised using 0.5 g L^{-1} trypsin containing 0.02 g L^{-1} EDTA (cat# FG301-01, TransGen). Trypsinization was stopped by adding heat-inactivated FBS. Cells were centrifuged (5 min, 300 × g) and resuspended in phosphate buffer and stored at 4 °C for at least 24 h.

We established the SCmic model in 24-well plates containing 1 mL of 1.5% agar per well, the model was built by mixing and exposing GMHA (1% w v^{-1} in phosphate buffer) contain nonviable cells (1×10^8 cells mL^{-1}, 90% HaCaT cells and 10% sebaceous cells) to UV light (405 nm, 60 s exposure) in the presence of the photoinitiator lithium phenyl (2,4,6-trimethylbenzoyl) phosphinate (cat# L157759, Aladdin, 0.3% w v^{-1}).

Construction of Hcm community

Cutibacterium acnes (*C. acnes*, ATCC 6919) was cultured anaerobically in RCM medium (cat# M5603B, TOPBIO) at 37 °C for 48 h, *Staphylococcus epidermidis* (*S. epidermidis*, CICC 10398) and *Staphylococcus aureus* (*S. aureus*, CICC 26003) was cultured in LB medium (cat# HB0128, hopebiol) at 37 °C. After centrifugation (10 minutes at 6200 × *g*), the bacteria were resuspended in a phosphate buffer and seeded at a density of 10^4-10^9 CFU cm^{-2} in the SCmic model. The Hcm community comprised of *Cutibacterium acnes*, *Cutibacterium granulosum*, *Staphylococcus epidermidis*, *Staphylococcus capitis*, *Corynebacterium simulans*, *Staphylococcus aureus*, and *Malassezia furfur*. Each strain was inoculated from a frozen stock solution into the appropriate liquid medium and was regularly passaged every 24 or 48 h. Prior to combining the individually cultured strains, each strain was rinsed at least three times using a PBS solution. They were then mixed according to the proportions specified in Supplementary Table 2. Please refer to Supplementary Table 2 for detailed strain information, which also includes primer sequences and their corresponding quantitative standard curves.

Preparation of HMb

Microbiota samples were collected from 10 cm^2 of the facial skin of a healthy volunteer by swabbing with swabs contain PBS and 2% polysorbate 80 (pH 7.0)[53]. Prior to participation, all subjects provided informed consent, and the experiments adhered to the ethical guidelines outlined in the WMA Declaration of Helsinki. The study was approved by the research ethics committee at the Third Affiliated Hospital of Nanjing Medical University (approval number: 2024-SR-056). Volunteers were expected not to clean or wear make up within 24 h before swabbing. The swabs were then transferred to 1.5 mL tubes containing 1 mL of PBS. After vortexing for 5 minutes and centrifuging for 5 minutes at 6200 × *g*, the samples were resuspended in a phosphate buffer. Subsequently, 20 µL of the buffer was spotted onto each model. The models were incubated at 32 °C and 75% relative humidity. To collect microbiota samples for 16S rRNA PMA-Illumina sequencing, the models were placed in 15 mL centrifuge tubes and 6 mL of PBS buffer was added. After vortexing for 30 minutes to elute the samples, they were collected for further analysis.

Skin type classification was based on sebum and water measurements[54], categorized as follows: oily type (Sebumeter: >66 µg cm^{-2}, Corneometer: >40 c.u.); normal type (Sebumeter: 33–66 µg cm^{-2}, Corneometer: >40 c.u.); dry type (Sebumeter: <33 µg cm^{-2}, Corneometer: <30 c.u.). The amount of facial sebum secretion was measured using the Sebumeter® (cat# SM 815, Courage + Khazaka Electronic), and water content was measured using the Corneometer® (cat# CM 825, Courage + Khazaka Electronic). Sebum and moisture measurement data are provided in Supplementary Table 3.

Morphology of model analysis

The surface morphology of the SCmic model were observed with an inverted optical microscope (cat# MF53-N, Mshot). The characteristics of the SCmic model were observed with field emission scanning electron microscope (SEM, cat# S4800, HITACHI) after freeze-dried.

Biofilm bacterial SEM analysis

After incubating *C. acnes* inoculated at about 1×10^7 CFU cm^{-2} at 32 °C for 48 h, we freeze-dried the SCmic model and took images of microbial colonization on the model using SEM.

Fluorescence staining for biofilm viability

3D model inoculated with *C. acnes* were cultured on 10 mm glass bottomed imaging dishes (cat# JGGJM-10, Solarbio) for 72 h at 37°C, bacteria and cells were stained with calcein AM (2 µM in PBS) for 45 min and PI (8 µM) for 10 min (cat# EFL-CLD-001, Suzhou Yongqinquan Intelligent Equipment Co., Ltd.). In principle, bacteria with intact cell membranes stain fluorescent green by calcein AM (Ex/EM: 495 nm/520 nm), while nonviable cells stain fluorescent red by PI (Ex/EM: 530 nm/620 nm).

16S rRNA fluorescence in situ hybridization (FISH)

3D model inoculated with *C. acnes*, *S. aureus* and *S. epidermidis* were cultured on 10 mm glass bottomed imaging dishes for 72 h at 32°C. FISH was used to detect the distribution characteristics of these three bacteria in the SCmic model. Bacteria were identified using the protocol described by Jordana-Lluch E et al.[13] with some modifications.

C. acnes, *S. aureus* and *S. epidermidis* were identified by the specific probes [5′ Cy3-CGGTAATGGGTAAAGAA-3′, 5′ Cy5-GAAG CAAGCTTCTCGTCCG-3′ and 5′ 6-FAM-ACTCTATCTCTAGAGGGGTCA G-3′, respectively][13,55,56]. To further partially permeabilize the model on glass-bottomed, fixed by absolute methanol for 3 min and dried at 37°C. Bacterial biofilm cells were permeabilized with 10 min incubation in 1 mg mL^{-1} proteinase K (cat# 19131, Qiagen) at 40°C, a methanol rinse for inactivation, and 10 min incubation with 1 mg mL^{-1} lysozyme (cat# DE103-01, Vazyme) at 40°C.The biofilms were rinsed with ultrapure water and dehydrated using 50%, 75%, and 100% ethanol for 2 minutes each. Prior to hybridization, the models were treated with hybridization buffer (6×SSC, 0.5% SDS, 100 µg mL^{-1} Salmon sperm DNA, and 50% Formamide). The hybridization buffer was incubated with the models in a 75°C-water bath for 10 minutes, followed by further incubation at 37°C for 60 minutes in a humid chamber. Specific probes for *C. acnes*, *S. aureus*, and *S. epidermidis* were added to the hybridization buffer at a concentration of 2 µM. The buffer containing the probes was then applied to each model, and the models were placed in glass-bottomed imaging dishes and incubated at 47°C in a humid chamber for 12 h.

After hybridization, the models were incubated with washing buffer (20 mM Tris–HCL buffer, pH 7.5, 0.64 M NaCl and 0.02% w v^{-1} SDS) for 20 min at 47°C. Washing action was stopped by rinsing of phosphate buffer. The samples were stained with DAPI (cat# D9542, Sigma) as a final stage.

Confocal laser scanning microscope

Fluorescent images were observed with confocal laser scanning microscope (CLSM, cat# LSM800, Zeiss) and processed using the ZEN imaging software. The sections of model were scanned through the full depth using appropriate settings for double- or triple-channel fluorescence recordings of 6′FAM, CY5, CY3, PI or AM. To eliminate spectral overlap between probes of multi-channel recordings, fluorochromes were scanned sequentially.

Images were captured in a 2D projection, Z-stack images taken at 0.85 µm intervals across a model and 3D reconstructions were performed using ZEN imaging software.

Measurement of the oxygen gradients within SCmic

The SCmic model was constructed in a confocal dish, followed by the addition of methylene blue (10 µM, cat# M190219, Aladdin). The model was then incubated in a normoxic chamber at 32 °C for 24 h. Fluorescent images of the SCmic were captured using a CLSM with Z-stack scanning.

Propidium monoazide (PMA)-quantitative PCR (qPCR) analysis

The precise determination of microorganism abundance in samples is enabled by Quantitative PCR (qPCR), or real-time PCR, which is used to quantify DNA by amplifying specific sequences and measuring amplification in real time.

To eliminate microbial genomic DNA (gDNA) originating from nonviable bacteria, collected bacteria were treated with propidium monoazide (PMA, cat# MX4220-1MG, MKBio) following the method of van et al. [14]. PCR amplification of gDNA from non-viable bacteria was performed after restaining the bacteria using a combination of bacteria collection and PMA treatment, followed by exposure to light. The bacteria were collected from the model and resuspended in 500 µL of PBS. Subsequently, 10 µL of PMA (20 µM) was added to the suspension. After incubating for 10 minutes in the dark, the samples were exposed to light from a 500 W halogen light source at a distance of 20 cm for 5 minutes. To prevent overheating, the cultures were kept on ice during the light exposure.

The samples were then centrifuged for 5 min at 6200 × *g*, and microbial gDNA was extracted using the QIAamp DNA Mini kit (cat# 51304, Qiagen). Microbial gDNA was used as template for qPCR amplification with ChamQ SYBR qPCR Master Mix (Low ROX Premixed) (cat# Q331-02, Vazyme) using the Bio-Rad CFX Connect apparatus. The design of strain-specific primers is given in Supplementary Table 2. By generating standard curves from known concentrations (Supplementary Table 2), we were able to accurately measure the absolute abundance of each microorganism.

Skin microbiota 16S rRNA gene sequencing analysis

Microbiota were collected from the model, treated with PMA, and genomic DNA was extracted using the QIAamp DNA Mini Kit. DNA concentration and quality were assessed with a NanoDrop spectrophotometer (cat# NC2000, Thermo Fisher Scientific) and verified via agarose gel electrophoresis.

The V3–V4 region of the 16S rRNA gene was amplified using primers 338 F (5′-ACTCCTACGGGAGGCAGCA-3′) and 806 R (5′-GGACTACHVGGGTWTCTAAT-3′) with sample-specific 7-bp barcodes. PCR reactions included 5× buffer, Fast Pfu DNA polymerase, dNTPs, primers, template DNA, and ddH_2O. Cycling conditions were 98 °C for 5 min, followed by 25 cycles of 98 °C for 30 s, 53 °C for 30 s, and 72 °C for 45 s, with a final extension at 72 °C for 5 min.

PCR amplicons were purified using Vazyme VAHTS DNA Clean Beads (cat# N411-01, Vazyme) and quantified with the Quant-iT PicoGreen dsDNA Assay Kit (cat# P7589, Invitrogen). Equal amounts of amplicons were pooled and sequenced (paired-end 2×250 bp) on an Illumina NovaSeq 6000 platform at Shanghai Personal Biotechnology Co., Ltd (Shanghai, China). Sequence data were submitted to NCBI (PRJNA 1193278).

Bioinformatics analysis was performed using QIIME2 (2022.11)[57]. Raw reads were demultiplexed, trimmed (cutadapt)[58], and processed via DADA2 for quality filtering, denoising, merging, and chimera removal[59]. Non-singleton amplicon sequence variants (ASVs) were aligned (MAFFT)[60] and used to construct a phylogenetic tree (FastTree2)[61]. Alpha diversity (Chao1 and Shannon[62,63]) and beta diversity metrics (weighted UniFrac[64]) metrics were calculated, with samples rarefied to 24715 sequences per sample. Taxonomy was assigned using the classify-sklearn naïve Bayes classifier[65] against the Greengenes Database (13.8).

Sequence analyses were conducted using the GenesCloud platform (https://www.genescloud.cn/home) with QIIME2 (2022.11) and R (v3.2.0). Alpha diversity indices (Chao1, Shannon) were calculated from the ASV table in QIIME2 and visualized as box plots. Ranked abundance curves assessed ASV richness and evenness. Beta diversity analysis, based on weighted Unifrac distance metrics[64], was visualized through principal coordinate analysis (PCoA) and unweighted pair-group method with arithmetic means (UPGMA) hierarchical clustering[66]. Differentially abundant taxa among groups were identified using LEfSe (Linear Discriminant Analysis Effect Size) with default parameters[67]. The similarity and differences in microbiota structure among groups were further assessed via weighted Unifrac distance analysis and evaluated using ANOSIM (Analysis of Similarities) in QIIME2[68].

Detection of microbial metabolism of arbutin

The skin-derived microbiota was inoculated on the SCmic model and then cultivate at 32 °C and 75% RH for 48 h. After 24 h of culturing, 50 µL of arbutin (cat# 03338, Sigma, 20 mg mL^{-1}, dissolved in PBS, pH 7.0) and nicotinamide solution (cat# 72340, Sigma, 30 mg mL^{-1}, dissolved in PBS, pH 7.0) were added, respectively. Without inoculating microbiota, arbutin and nicotinamide solution were added directly to the model as blank control. The reaction samples were collected by placing the model in a 15 mL centrifuge tube, adding 1 mL of anhydrous methanol, vortexing for 30 min to elute, and centrifuging at 6200 × g for 5 min. The supernatant was subsequently analyzed using a high-performance liquid chromatography (HPLC, cat# Nexera XR LC-20AD XR, Shimadzu). The detailed mobile phase procedure is shown in Supplementary Table 4.

Molecular modeling

Molecular docking was performed using CB-Dock2[69]. The structures of the drug compounds were retrieved from the PubChem database, the FASTA sequence of the target protein was obtained from the National Center for Biotechnology Information (NCBI). In addition, the 3D structures of the protein were generated through homology modeling using Swiss-Modeler[70].

Hydrogel rheological analysis

The elastic modulus, which measures gel stiffness, was assessed using a rheometer (cat# MCR 102, Anton-Paar). The storage modulus (G′) and loss modulus (G″) were measured at a frequency of 1 Hz and a constant shear strain of 0.4% at 37°C.

Reporting summary

Further information on research design is available in the Nature Portfolio Reporting Summary linked to this article.

Data availability

The sequence data analyzed during the current study are available from NCBI (PRJNA 1193278, http://www.ncbi.nlm.nih.gov/bioproject/1193278). All data are available in the main text or the Supplementary Information/Source Data file. Source data is available for Figs. 1e, g, h, 2a-d, f, g, 3b-i, 4b-e, 5b-d, g, h, i and 6b, e and Supplementary Figs. 2, 3, 4, 5, 6 and 7 in the associated source data file. Source data are provided with this paper.

References

1. Scharschmidt, T. C. & Fischbach, M. A. What lives on our skin: ecology, genomics and therapeutic opportunities of the skin microbiome. *Drug Discov. Today Dis. Mechanisms* **10**, e83–e89 (2013).
2. Byrd, A. L., Belkaid, Y. & Segre, J. A. The human skin microbiome. *Nat. Rev. Microbiol.* **16**, 143–155 (2018).
3. Williams, H. C., Dellavalle, R. P. & Garner, S. Acne vulgaris. *Lancet* **379**, 361–372 (2012).
4. Zhang, E. et al. Characterization of the skin fungal microbiota in patients with atopic dermatitis and in healthy subjects. *Microbiol. Immunol.* **55**, 625–632 (2011).
5. Zheng, Y. et al. Skin microbiome in sensitive skin: The decrease of Staphylococcus epidermidis seems to be related to female lactic acid sting test sensitive skin. *J. dermatological Sci.* **97**, 225–228 (2020).
6. Boxberger, M., Cenizo, V., Cassir, N. & La Scola, B. Challenges in exploring and manipulating the human skin microbiome. *Microbiome* **9**, 125 (2021).
7. Larson, P. J., Chong, D., Fleming, E. & Oh, J. Challenges in developing a human model system for skin microbiome research. *J. Investigative Dermatol.* **141**, 228–231 (2021).
8. Chen, L. et al. Skin and gut microbiome in psoriasis: Gaining insight into the pathophysiology of it and finding novel therapeutic strategies. *Front. Microbiol.* **11**, 589726 (2020).
9. Grice, E. A. et al. Topographical and temporal diversity of the human skin microbiome. *Science* **324**, 1190–1192 (2009).
10. Davies, C. E. et al. Use of molecular techniques to study microbial diversity in the skin: chronic wounds reevaluated. *Wound Repair regeneration: Off. Publ. Wound Healing Soc. Eur. Tissue Repair Soc.* **9**, 332–340 (2001).
11. Ide, K. et al. Exploring strain diversity of dominant human skin bacterial species using single-cell genome sequencing. *Front. Microbiol.* **13**, 955404 (2022).
12. Myles, I. A. et al. A method for culturing Gram-negative skin microbiota. *BMC Microbiol* **16**, 60 (2016).
13. Jordana-Lluch, E. et al. A simple polymicrobial biofilm keratinocyte colonization model for exploring interactions between commensals, pathogens and antimicrobials. *Front Microbiol* **11**, 291 (2020).
14. van der Krieken, D. A. et al. An in vitro model for bacterial growth on human stratum corneum. *Acta Derm. Venereol.* **96**, 873–879 (2016).
15. Bojarrichard, A. Studying the human skin microbiome using 3D in vitro skin models. *Appl. Vitr. Toxicol.* **1**, 165–171 (2015).
16. Pinto, D., Ciardiello, T., Franzoni, M., Pasini, F. & Rinaldi, F. Effect of commonly used cosmetic preservatives on skin resident microflora dynamics. *Sci. Rep.* **11**, 8695 (2021).
17. Jourdain, R. et al. Malassezia restricta-mediated lipoperoxidation: A novel trigger in dandruff. *Acta Derm.-venereologica* **103**, adv00868 (2023).
18. Sfriso, R., Egert, M., Gempeler, M., Voegeli, R. & Campiche, R. Revealing the secret life of skin - With the microbiome you never walk alone. *Int. J. Cosmet. Sci.* **42**, 116–126 (2020).
19. Duckney, P. et al. The role of the skin barrier in modulating the effects of common skin microbial species on the inflammation, differentiation and proliferation status of epidermal keratinocytes. *BMC Res. notes* **6**, 474 (2013).
20. Holland, K. T. & Bojar, R. A. Cosmetics: what is their influence on the skin microflora? *Am. J. Clin. Dermatol.* **3**, 445–449 (2002).
21. He, S. et al. Construction of a dual-component hydrogel matrix for 3D biomimetic skin based on photo-crosslinked chondroitin sulfate/collagen. *Int J. Biol. Macromol.* **254**, 127940 (2024).
22. Li, Z. et al. Characterization of the human skin resistome and identification of two microbiota cutotypes. *Microbiome* **9**, 47 (2021).
23. Masuda, Y. et al. Three-dimensional morphological characterization of the skin surface micro-topography using a skin replica and changes with age. *Ski. Res. Technol.: Off. J. Int. Soc. Bioeng. Ski. (ISBS) Int. Soc. Digital Imaging Ski. (ISDIS) Int. Soc. Ski. Imaging (ISSI)* **20**, 299–306 (2014).
24. Oh, J. et al. Temporal stability of the human skin microbiome. *Cell* **165**, 854–866 (2016).
25. Grice, E. A. & Segre, J. A. The skin microbiome. *Nat. Rev. Microbiol* **9**, 244–253 (2011).
26. Eckert, R. L. Structure, function, and differentiation of the keratinocyte. *Physiological Rev.* **69**, 1316 (1989).
27. McGinley, K. J., Webster, G. F. & Leyden, J. J. Regional variations of cutaneous propionibacteria. *Appl. Environ. Microbiol.* **35**, 62–66 (1978).
28. Brook, I. Antimicrobials therapy of anaerobic infections. *J. Chemother.* **28**, 143–150 (2016).
29. Akaza, N. et al. The microbiome in comedonal contents of inflammatory acne vulgaris is composed of an overgrowth of *Cutibacterium Spp*. and other cutaneous microorganisms. *Clin., Cosmet. investigational Dermatol.* **15**, 2003–2012 (2022).
30. Costello, E. K. et al. Bacterial community variation in human body habitats across space and time. *Science* **326**, 1694–1697 (2009).
31. Gan, B. et al. Dynamic monitoring of changes in fecal flora of giant pandas in mice: Co-occurrence network reconstruction. *Microbiol. Spectr.* **11**, e0199122 (2022).
32. Peng, X. et al. Poloxamer 407 and hyaluronic acid thermosensitive hydrogel-encapsulated ginsenoside Rg3 to promote skin wound healing. *Front. Bioeng. Biotechnol.* **10**, 831007 (2022).
33. González-Mondragón, E. A. et al. Acne and diet: a review of pathogenic mechanisms. *Boletin Med. del. Hospital Infant. de. Mex.* **79**, 83–90 (2022).
34. Harris-Tryon, T. A. & Grice, E. A. Microbiota and maintenance of skin barrier function. *Science* **376**, 940–945 (2022).
35. Shats, I. et al. Bacteria boost mammalian host NAD metabolism by engaging the deamidated biosynthesis pathway. *Cell Metab.* **31**, 564–579 (2020).
36. Yao, J. K. et al. Prevalence and specificity of the abnormal niacin response: A potential endophenotype marker in schizophrenia. *Schizophrenia Bull.* **42**, 369–376 (2016).
37. Eisenstein, M. The skin microbiome. *Nature* **588**, S209 (2020).
38. Human Microbiome Project Consortium. Structure, function and diversity of the healthy human microbiome. *Nature* **486**, 207-214 (2012).
39. Aranda-Díaz, A. et al. Establishment and characterization of stable, diverse, fecal-derived in vitro microbial communities that model the intestinal microbiota. *Cell host microbe* **30**, 260–272 (2022).
40. Fukuda, K. et al. Three stepwise pH progressions in stratum corneum for homeostatic maintenance of the skin. *Nat. Commun.* **15**, 4062 (2024).
41. Grice, E. A. et al. A diversity profile of the human skin microbiota. *Genome Res.* **18**, 1043–1050 (2008).
42. Jin, Z., Song, Y. & He, L. A review of skin immune processes in acne. *Front. Immunol.* **14**, 1324930 (2023).
43. Ma, L. et al. The characteristics of the skin physiological parameters and facial microbiome of "Ideal Skin" in Shanghai women. *Clin. Cosmet. Investigational Dermatol.* **16**, 325–337 (2023).
44. Chen, Y., Knight, R. & Gallo, R. L. Evolving approaches to profiling the microbiome in skin disease. *Front Immunol.* **14**, 1151527 (2023).

45. Claudel, J. P. et al. Staphylococcus epidermidis: A potential new player in the physiopathology of acne? *Dermatology* **235**, 287–294 (2019).
46. Koppel, N., Maini Rekdal, V. & Balskus, E. P. Chemical transformation of xenobiotics by the human gut microbiota. *Science* **356**, 6344 (2017).
47. Smit, N., Vicanova, J. & Pavel, S. The hunt for natural skin whitening agents. *Int. J. Mol. Sci.* **10**, 5326–5349 (2009).
48. Bang, S. H., Han, S. J. & Kim, D. H. Hydrolysis of arbutin to hydroquinone by human skin bacteria and its effect on antioxidant activity. *J. Cosmet. Dermatol.* **7**, 189–193 (2008).
49. Snaidr, V. A., Damian, D. L. & Halliday, G. M. Nicotinamide for photoprotection and skin cancer chemoprevention: A review of efficacy and safety. *Exp. Dermatol.* **28**, 15–22 (2019).
50. Cheng, A. G. et al. Design, construction, and in vivo augmentation of a complex gut microbiome. *Cell* **185**, 3617–3636 (2022).
51. Baier Leach, J. et al. Photocrosslinked hyaluronic acid hydrogels: natural, biodegradable tissue engineering scaffolds. *Biotechnol. Bioeng.* **82**, 578–589 (2003).
52. Thiboutot, D. et al. Human skin is a steroidogenic tissue: steroidogenic enzymes and cofactors are expressed in epidermis, normal sebocytes, and an immortalized sebocyte cell line (SEB-1). *J. Invest Dermatol* **120**, 905–918 (2003).
53. Akaza, N. et al. Microorganisms inhabiting follicular contents of facial acne are not only *Propionibacterium* but also *Malassezia spp*. *J. Dermatol.* **43**, 906–911 (2016).
54. Youn, S. W. et al. Evaluation of facial skin type by sebum secretion: discrepancies between subjective descriptions and sebum secretion. *Ski. Res. Technol.: Off. J. Int. Soc. Bioeng. Ski. (ISBS) Int. Soc. Digital Imaging Ski. (ISDIS) Int. Soc. Ski. Imaging (ISSI)* **8**, 168–172 (2002).
55. Jahns, A. C. et al. Simultaneous visualization of *Propionibacterium acnes* and *Propionibacterium granulosum* with immunofluorescence and fluorescence in situ hybridization. *Anaerobe* **23**, 48–54 (2013).
56. Zakrzewska-Czerwińska, J. et al. Identification of Staphylococcus epidermidis using a 16S rRNA-directed oligonucleotide probe. *FEMS Microbiol Lett.* **100**, 51–58 (1992).
57. Bolyen, E. et al. QIIME 2: Reproducible, interactive, scalable, and extensible microbiome data science. *PeerJ Prepr.* **6**, e27295v2 (2018).
58. Marcel, M. Cutadapt removes adapter sequences from high-throughput sequencing reads. *EMBnet* **17**, pp–10 (2011).
59. Callahan, B. J. et al. Dada2: high-resolution sample inference from illumina amplicon data. *Nat. Methods* **13**, 581–583 (2016).
60. Katoh, K. Mafft: a novel method for rapid multiple sequence alignment based on fast fourier transform. *Nucleic Acids Res.* **30**, 3059–3066 (2002).
61. Price, M. N., Dehal, P. S. & Arkin, A. P. FastTree: computing large minimum evolution trees with profiles instead of a distance matrix. *Mol. Biol. Evol.* **26**, 1641–1650 (2009).
62. Chao, A. Nonparametric estimation of the number of classes in a population. *Scand. J. Stat.* **11**, 265–270 (1984).
63. Shannon, C. E. A mathematical theory of communication. *Bell Syst. Tech. J.* **27**, 379–423 (1948).
64. Lozupone, C. A. et al. Quantitative and qualitative beta diversity measures lead to different insights into factors that structure microbial communities. *Appl Environ. Microbiol* **73**, 1576–1585 (2007).
65. Bokulich, N. A. et al. Optimizing taxonomic classification of marker-gene amplicon sequences with QIIME 2's q2-feature-classifier plugin. *Microbiome* **6**, 90 (2018).
66. Ramette, A. Multivariate analyses in microbial ecology. *FEMS Microbiol Ecol.* **62**, 142–160 (2007).
67. Segata, N. et al. Metagenomic biomarker discovery and explanation. *Genome Biol.* **12**, R60 (2011).
68. Clarke, K. R. Non-parametric multivariate analyses of changes in community structure. *Aust. J. Ecol.* **18**, 117–143 (1993).
69. Liu, Y. et al. CB-Dock2: improved protein-ligand blind docking by integrating cavity detection, docking and homologous template fitting. *Nucleic acids Res.* **50**, W159–w164 (2022).
70. Waterhouse, A. et al. SWISS-MODEL: homology modelling of protein structures and complexes. *Nucleic acids Res.* **46**, W296–w303 (2018).

Acknowledgements

This work was financially supported by the China Pharmaceutical University (Grant No. 3150020057 to Q.H.).

Author contributions

Q.H., J.W., and P.W. conceived and designed the project. P.W., H.L., and J.W. wrote the manuscript. P.W., J.W., Y.G., X.H.F.C., and Q.H. provided edits to the manuscript. P.W., H.L., J.X.Z., X.W., W.S., and Y.X.Z. performed the experiments. H.L. and B.C. provided experimental support. P.W., J.W., and Q.H. performed the computational and statistical analyses.

Competing interests

The authors declare no competing interests.

Additional information

Supplementary information The online version contains supplementary material available at https://doi.org/10.1038/s41467-025-58377-2.

Correspondence and requests for materials should be addressed to Jianxin Wu or Qing Huang.

Peer review information *Nature Communications* thanks Hasan Abaci, who co-reviewed with Alberto PappalardoJagir (R) Hussan; and Ana Porras for their contribution to the peer review of this work. A peer review file is available.